Journal of Applied Polymer Science

# Synthesis and Optical Properties of POSS-Based Oxadiazole Nanohybrids with Three-Dimensional Molecular Conjugated Structure

**Yongxin Yan,[1] Jun Wang,[2] Tianbao Liu,[1] Xin Wang,[1,2] Xinyan Su,[3] Yan Feng[2]**

[1]School of Materials and Chemical Engineering, Chizhou University, Chizhou 247000, China
[2]School of Chemistry and Chemical Engineering, Anhui University, Hefei 230039, China
[3]School of Materials Science and Engineering, Shanghai University, Shanghai 200072, China
Correspondence to: X. Wang (E-mail: wangxin164@sina.com) or Y. Feng (E-mail: fy70@163.com)

**ABSTRACT:** A series of oxadiazole-containing molecular hybrid materials with three-dimensional structure (**P1–P3**) was prepared by Heck reaction based on the octavinylsilsesquioxane. All resultant hybrid materials are soluble in common organic solvents and possess good film-forming property. Their structures and properties were characterized and evaluated by FTIR, $^{1}$H-NMR, $^{13}$C-NMR, $^{29}$Si-NMR, MALDI-TOF, UV–vis, photoluminescence (PL), cyclic voltammetry, and elemental analysis (EA). The results showed that the substituted arm numbers of hybrids (**P2** and **P3**) with pushing electron groups were efficiently controlled. Moreover, the hybrids possessed a steady blue emission and good electron-injecting property in film. © 2013 Wiley Periodicals, Inc. J. Appl. Polym. Sci. **2014**, *131*, 40246.

**KEYWORDS:** optical properties; electrochemistry; composites

Received 10 August 2013; accepted 1 December 2013
**DOI: 10.1002/app.40246**

## INTRODUCTION

Organic semiconductors have been extensively studied and used in light-emitting diode (LED) applications.[1] However, the fabrication of LED by using organic dye materials involves relatively expensive techniques such as sublimation or vapor deposition,[2] and the small organic molecules can readily aggregate in solid phase.[3] Much effort has been done to overcome the problems.[4,5] The molecules with three-dimensional (3D) structure, such as tetrahedranes, cubanes, and star molecules, provide an alternative way.[6,7] Nevertheless, to our knowledge, few molecular structures offer perfect (cubic) symmetry in three dimensions and octafunctionality such that each octant in Cartesian space contains one functional group.[7] The cubane family is relatively difficult to be prepared; however, the functional cubic oligomeric silsesquioxane (POSS) materials are easily obtained.[8,9] POSS is a type of three-dimensional, structurally well-defined cage molecule with the general formula $(RSiO_{1.5})_n$, and typical POSS derivatives have the structure of a cube-octameric framework covalently bonded with eight organic groups.[10–12] Therefore, the functionalized POSSs have the potential to assemble 2D or 3D macroscopic structures in nanometer[13–15] and possess some unique properties, including good optical and electrical properties and excellent film-forming properties as well as moisture resistance.[10,16–19]

In general, the hybrid materials with rigid conjugated linkage between organic functionalized groups and POSS are prepared by using Karstedt catalyst[20–22]; however, the steric effect limited the arm numbers of the hybrids.[21,23–25] An alternate strategy is to choose the Suzuki coupling reaction or the Heck reaction by the use of octavinylsilsesquioxane (OVS) as cubic building blocks for weakening the steric effect.[26] Nevertheless, Zhang and coworkers[27] reported that the Suzuki coupling did not work well for the synthesis of the quantum dot-like organic–inorganic clusters. Sellinger et al.[16,28] obtained a mixture of 3–10 substituted compounds via the Heck reaction between OVS and haloaromatic compounds. The propensity for substitutions was studied by MALDI-TOF, and the results showed that these products were of lower purity, most of which had more than five types of substitutions.

Here, we designed and synthesized a series of POSS-based nanohybrids (**P1–P3**) with the OVS core that combined the organic molecular component (oxadiazole unit) by the covalent bond to form a rigid link (Scheme 1). The influence of different terminal groups on the substituted arm numbers of hybrids was mainly investigated. It was expected that the hybrids with the perfect symmetry structure in three dimensions by the variety of substituent groups will be obtained. In addition, the optical and electrical properties of hybrids were evaluated in detail.

## EXPERIMENTAL

### Materials

OVS was purchased from Shengyan Meixi Chemical Company (Shengyan, China). $Pd(PPh_3)_2Cl_2$ was purchased from Aldrich.

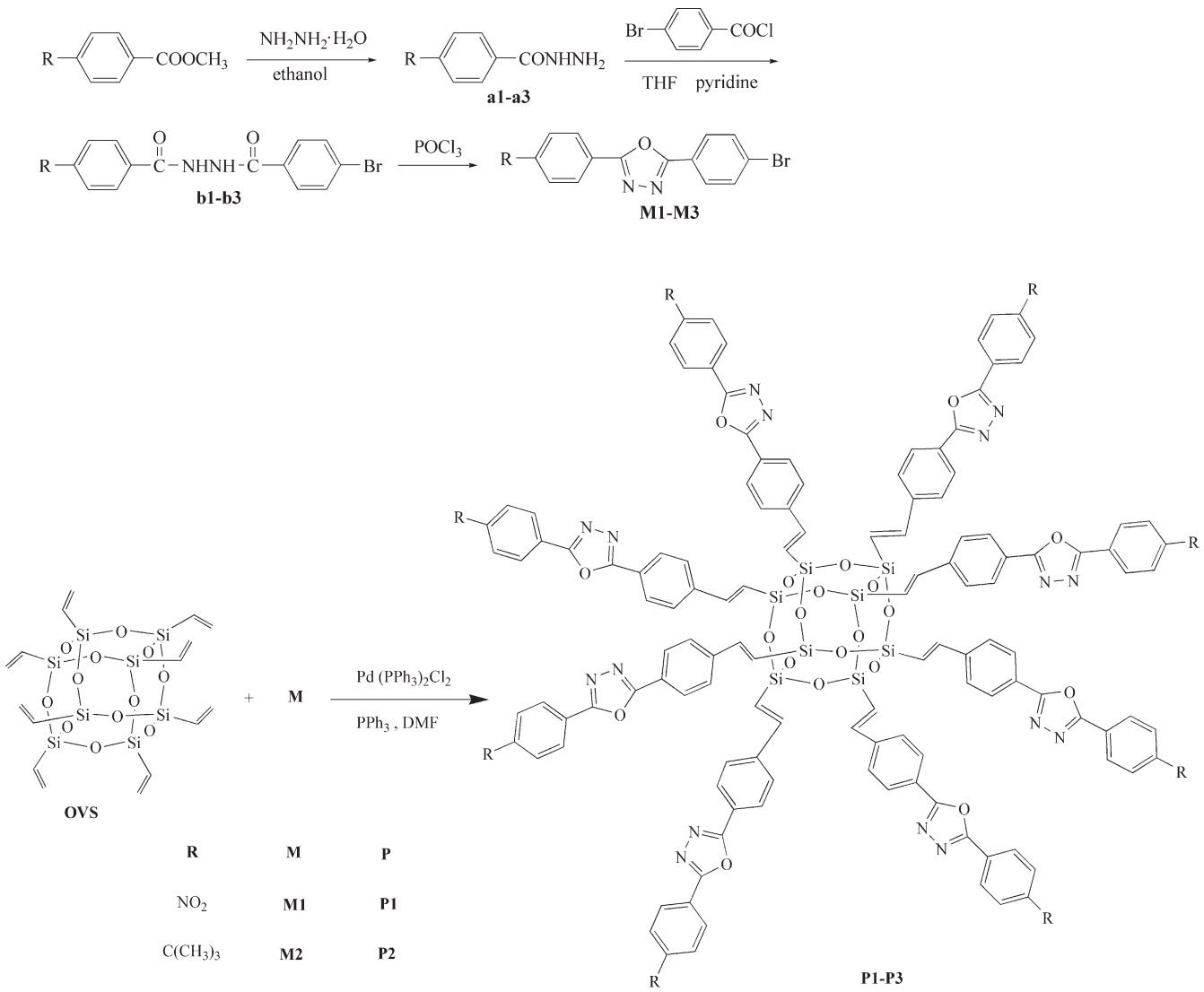


**Scheme 1.** Preparation of **M1–M3** and **P1–P3**.

All other chemicals were purchased from Shanghai Reagent (Shanghai, China) and used as received.

### Instrumentation

FTIR spectra were recorded on a Nicolet IS10 FTIR spectrometer with KBr pellets. $^{1}$H-NMR, $^{13}$C-NMR, and $^{29}$Si-NMR spectra were obtained with a AVANCE/DMX 400 MHz Bruker NMR spectrometer. MALDI-TOF was performed on a Bruker Autoflex MALDI-TOF mass spectrometer. The UV–vis and PL spectra were measured on a Hitachi U-3900 spectrometer and a Shimadzu RF-5301 spectrometer, respectively. Quantum yields ($\Phi_f$) were determined by using a dilute quinine sulfate in 0.10 mol $L^{-1}$ $H_2SO_4$ as the standard ($\Phi_f = 0.546$).[29] Cyclic voltammetry (CV) was performed using a LK2005 electrochemical analyzer with a three-electrode cell in a solution of $(n\text{-Bu})_4NClO_4$ (0.1 mol $L^{-1}$) in acetonitrile at a scanning rate of 50 mV $s^{-1}$. A thin film of the hybrid was coated onto the working electrode (glass–carbon) by dipping the electrode into a solution of the hybrid.[30] The coated electrode was dried in a vacuum oven at 40°C, resulting in a thin film on the work electrode. A Pt wire was used as a counter electrode, and an $Ag/Ag^{+}$ (0.10 mol $L^{-1}$ in $CH_3CN$) electrode was used as a reference electrode.

### Synthesis of Monomers (M1–M3)

**M1** and **M2** were prepared by following the literature procedure with slight modification.[31–33] **M3** was synthesized according to the method proposed in Ref. 34.

**General Procedure for the Synthesis of Benzoyl Hydrazine (a1–a3).** A mixture of appropriate benzoate (0.133 mol) and excess hydrazine monohydrate (0.500 mol) was refluxed for 24 h. The reaction mixture was cooled and then collected by recrystallizing from ethanol, and then the corresponding hydrazine (**a1–a3**) was obtained.

**a1**: Yield: 89%. FTIR (KBr, $cm^{-1}$): 3334, 3264 (N—*H*); 3068 (=CH); 1642 (C=O); 1618, 1597, 1507 (Ar); 847 (*p*-Ar). $^{1}$H-NMR (400 MHz, DMSO-$d_6$, $\delta$, ppm): 4.30 (s, 2H, $NH_2$), 7.94

(d, 2H, $J = 8.0$ Hz, Ar-*H*), 8.34 (d, 2H, $J = 8.0$ Hz, Ar-*H*), 9.41 (s, 1H, N*H*).

**a2**: Yield: 87%. FTIR (KBr, $cm^{-1}$): 3500–3100 (N—*H*); 3055 (=CH); 2960, 2870 ($CH_3$); 1628 (C=O); 1563 (Ar); 1536 (N—H); 857 (*p*-Ar). $^1$H-NMR (400 MHz, DMSO-$d_6$, $\delta$, ppm): 1.31 [s, 9H, C($CH_3$)$_3$], 4.49 (s, 2H, $NH_2$), 7.45 (d, 2H, $J = 8.3$ Hz, Ar-*H*), 7.75 (d, 2H, $J = 8.3$ Hz, Ar-*H*), 9.69 (s, 1H, N*H*).

**a3**: Yield: 87%. FTIR (KBr, $cm^{-1}$): 3320, 3180 (N—H); 2918, 2855 ($CH_2$, $CH_3$); 1647 (C=O); 1617, 1506 (Ar); 836 (*p*-Ar). $^1$H-NMR (400 MHz, DMSO-$d_6$, $\delta$, ppm): 0.84 (t, 3H, $CH_3$), 1.35 [m, 10H, ($CH_2$)$_5$], 1.68 (m, 2H, $CH_2CH_2O$), 3.9 (t, 2H, $CH_2O$), 4.4 (s, 2H, $NH_2$), 6.94 (d, 2H, $J = 8.8$ Hz, Ar-*H*), 7.75 (d, 2H, $J = 8.8$ Hz, Ar-*H*), 9.57 (s, 1H, N*H*$NH_2$).

**General Procedure for the Synthesis of Benzoyl Hydrazine (b1–b3).** 4-Bromobenzoic acid (0.10 mol) in 150 mL anhydrous toluene was added to 100 mL of $SOCl_2$ and refluxed for 6 h to give 4-bromobenzoyl chloride. The excess $SOCl_2$ was removed by vacuum distillation, and the reaction mixture was cooled to room temperature. Compound **a** (0.10 mol) was dissolved in 200 mL of THF and 50 mL of pyridine and then added to the reaction flask containing 4-bromobenzoyl chloride over a period of 20 min in an ice bath. After being stirred for 3 h, the reaction mixture was poured into distilled water. The product was collected on a filter and washed with water and then dried in a vacuum oven.

**b1**: Yield: 81%. FTIR (KBr, $cm^{-1}$): 3199 (N—*H*); 3015 (=CH); 2831 ($CH_2$); 1793, 1720 (C=O); 1602, 1589, 1561 (Ar); 837 (*p*-Ar). $^1$H-NMR (400 MHz, DMSO-$d_6$, $\delta$, ppm): 7.79 (d, 2H, $J = 8.0$ Hz, Ar-*H*), 7.88 (d, 2H, $J = 8.0$Hz, Ar-*H*), 8.15 (d, 2H, $J = 8.0$ Hz, Ar-*H*), 8.36 (d, 2H, $J = 8.0$ Hz, Ar-*H*), 10.75 (s, 1H, N*H*), 10.92 (s, 1H, N*H*).

**b2**: Yield: 71%. FTIR (KBr, $cm^{-1}$): 3409, 3283 (N—H); 3062, 3026 (=CH); 2960, 2867 ($CH_3$); 1687, 1642 (C=O); 1613, 1590 (Ar); 1544, 1518 (N—H); 847 (*p*-Ar). $^1$H-NMR (400 MHz, DMSO-$d_6$, $\delta$, ppm): 1.31 [s, 9H, C($CH_3$)$_3$], 7.54 (d, 2H, $J = 8.4$ Hz, Ar-*H*), 7.75 (d, 2H, $J = 8.4$ Hz, Ar-*H*), 7.84 (d, 2H, $J = 9.0$ Hz, Ar-*H*), 7.88 (d, 2H, $J = 9.0$ Hz, Ar-*H*), 10.47 (s, 1H, N*H*), 10.60 (s, 1H, N*H*).

**b3**: Yield: 81%. FTIR (KBr, $cm^{-1}$): 3206 (N—H); 2922, 2825 ($CH_2$, $CH_3$); 1700, 1750 (C=O); 1603, 1460 (Ar); 828 (Ar).$^1$H-NMR (400 MHz, DMSO-$d_6$, $\delta$, ppm): 0.87 (t, 3H, $CH_3$), 1.42 [m, 10H, ($CH_2$)$_5$], 1.75 (m, 2H, $CH_2CH_2O$), 4.05 (t, 2H, $CH_2O$), 7.03 (d, 2H, $J = 8.7$ Hz, Ar-*H*), 7.75 (d, 2H, $J = 8.4$Hz, Ar-*H*), 7.88 (m, 4H, Ar-*H*), 10.31 (s, 1H, N*H*), 10.45 (s, 1H, N*H*).

**General Procedure for the Synthesis of Monomers (M1–M3).** The mixture of Compound **b** (0.067 mol) and 300 mL of $POCl_3$ was refluxed for 12 h under nitrogen atmosphere. After the completion of the reaction, the reaction mixture was slowly poured into cold water, and then 0.5 mol $L^{-1}$ NaOH solution was added to neutralize the reaction mixture. Then, the precipitate was filtered and washed with distilled water. The product was collected by recrystallizing from ethanol/water = 3 : 1 (v/v).

**M1**: Yield: 96%. FTIR (KBr, $cm^{-1}$): 3058 (=CH); 1601, 1528, 1475 (Ar); 837 (*p*-Ar). $^1$H-NMR (400 MHz, $CDCl_3$, $\delta$, ppm): 7.74 (d, 2H, $J = 8.4$ Hz, Ar-*H*), 8.06 (d, 2H, $J = 8.4$ Hz, Ar-*H*), 8.36 (d, 2H, $J = 9.2$ Hz, Ar-*H*), 8.44 (d, 2H, $J = 8.8$ Hz, Ar-*H*). $^{13}$C-NMR (100 MHz, $CDCl_3$, $\delta$, ppm): 164.8, 163, 149.3, 132.7, 129, 126.7, 124.1, 122. Anal. Calcd for $C_{14}H_8O_3N_3Br$: C, 48.56; H, 2.31; N, 12.14; Found (%): C, 48.53; H, 2.30; N, 12.1.

**M2**: Yield: 79%. FTIR (KBr, $cm^{-1}$): 3061 (=CH); 2961, 2868 ($CH_3$); 1599 (Ar); 836 (*p*-Ar). $^1$H-NMR (400 MHz, $CDCl_3$, $\delta$, ppm): 1.37 [s, 9H, C($CH_3$)$_3$], 7.54 (d, 2H, $J = 8.5$ Hz, Ar-*H*), 7.67 (d, 2H, $J = 8.6$ Hz, Ar-*H*), 8.00 (d, 2H, $J = 8.6$ Hz, Ar-*H*), 8.04 (d, 2H, $J = 8.5$ Hz, Ar-*H*). $^{13}$C-NMR (100 MHz, $CDCl_3$, $\delta$, ppm): 164.2, 154.9, 132.4, 128.5, 126.5, 120.7, 68.7, 35.1, 30.7. Anal. Calcd for $C_{19}H_{17}ON_2Br$: C, 61.79; H, 4.61; N, 4.34; Found (%): C, 61.72; H, 4.60; N, 4.26.

**M3**: Yield: 85%. FTIR (KBr, $cm^{-1}$): 2922, 2853 ($CH_2$, $CH_3$); 1610, 1475 (Ar); 1255 (C—O—C); 829 (*p*-Ar). $^1$H-NMR (400 MHz, $CDCl_3$, $\delta$, ppm): 0.88 (t, 3H, $CH_3$), 1.40 [m, 10H, ($CH_2$)$_5$], 1.87 (m, 2H, $CH_2CH_2O$), 4.04 (t, 2H, $CH_2O$), 7.02 (d, 2H, $J = 8.9$ Hz, Ar-*H*), 7.68 (d, 2H, $J = 8.6$ Hz, Ar-*H*), 8.04 (m, 4H, Ar-*H*). $^{13}$C-NMR (100 MHz, $CDCl_3$, $\delta$, ppm): 162.4, 161.7, 132.4, 129.5, 118, 114, 69, 30.7, 29.6, 29.1, 26, 22.7, 14.1. Anal. Calcd for $C_{22}H_{25}O_2N_2Br$: C, 61.54; H, 5.83; N, 6.53; Found (%): C, 61.52; H, 5.86; N 6.50.

### Synthesis of Hybrids (P1–P3)

**General Procedure for the Synthesis of Hybrids.** Synthesis of hybrids (**P1–P3**) was according to Scheme 1. The Heck reaction was performed under nitrogen using Schlenk techniques in vacuum-line system.[35,36] To a 25-mL Schlenk tube with a side arm, 0.1 mmol OVS, 0.8 mmol monomer (the molar ratio of OVS and monomer is 1 : 8), 1.0 mg $Pd(PPh_3)_2Cl_2$, 10 mg $PPh_3$, 10 mL DMF, and 5 mL $Et_3N$ were added. The mixture was stirred at 110°C for 72 h. On completion, DMF was distilled under vacuum (75°C/36 mmHg), and then final purification was achieved by column chromatography [ethyl acetate/petroleum ether = 1 : 12 (v/v)].

**P1**: Bright yellow powder, yield: 41%. FTIR (KBr, $cm^{-1}$): 3068 (=CH); 1600, 1523, 1473, 1432 (Ar); 1132 (Si—O—Si); 850 (*p*-Ar). $^1$H-NMR (400 MHz, $CDCl_3$, $\delta$, ppm): 6.07 (br, Si—CH= and unreacting olefin proton), 6.91 (br, 7H, Ar-CH=), 7.63 (br, 42H, Ar-H), 8.56 (br, 14H, Ar-H). $^{13}$C-NMR (100 MHz, $CDCl_3$, $\delta$, ppm): 165, 148, 135, 132, 128, 127, 126, 125, 120, 96. $^{29}$Si-NMR (79.49 MHz, $CDCl_3$, $\delta$, ppm): −79.46 (Si—C), −81.27 (Si—C). Anal. Calcd for $C_{114}H_{72}O_{33}N_{21}Si_8$ (hept-substituted cube): C, 56.39; H, 2.97; N, 12.12; Found (%): C, 55.63; H, 2.97; N, 11.96.

**P2**: Yellow power, yield: 48%. FTIR (KBr, $cm^{-1}$): 3065 (=CH); 2850 ($CH_3$); 1599, 1476, 1462 (Ar); 1131 (Si—O—Si); 870 (*p*-Ar). $^1$H-NMR (400 MHz, $CDCl_3$, $\delta$, ppm): 1.33 [58.5H, C($CH_3$)$_3$], 6.08 (Si—CH= and unreacting olefin proton), 6.82 (6.5H, Ar-CH=), 7.74 (26H, Ar-H), 7.95 (26H, Ar-H). $^{13}$C-NMR (100 MHz, $CDCl_3$, $\delta$, ppm): 164, 157, 132, 127, 126, 123, 94, 39, 31. $^{29}$Si-NMR (79.49 MHz, $CDCl_3$, $\delta$, ppm): −79.66 (Si—C), −81.30 (Si—C). Anal. Calcd for $C_{142}H_{135}O_{19}N_{14}Si_8$ (hept-substituted cube): C, 66.48; H, 5.27; N, 7.65; Found (%): C, 63.74; H, 5.15; N, 7.27.

**P3**: Yellow power, yield: 45%. FTIR (KBr, $cm^{-1}$): 3065 (=CH); 2928, 2850 ($CH_2$, $CH_3$); 1602, 1476, 1431 (Ar); 1262

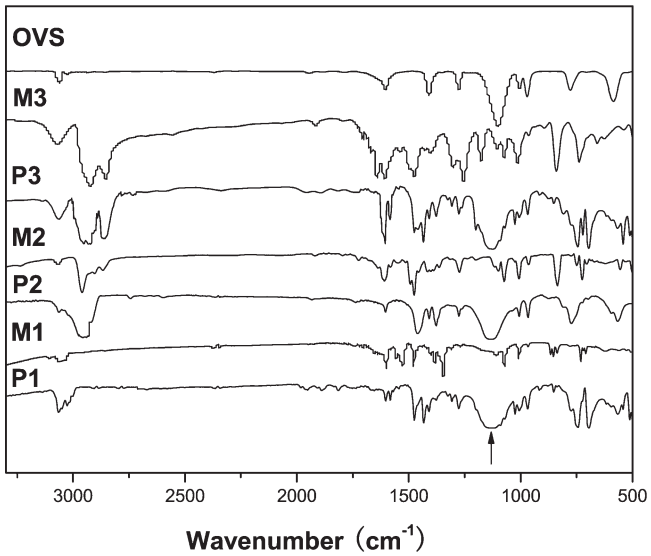


**Figure 1.** FTIR spectra of OVS, **M1–M3**, and **P1–P3**.

(C—O—C); 1131 (Si—O—Si); 855 (*p*-Ar). $^{1}$H-NMR (400 MHz, $CDCl_3$, $\delta$, ppm): 0.88 (20.1H, $CH_3$), 1.28 [67H, $(CH_2)_5$], 1.82 (13.4H, $CH_2CH_2O$), 4.03 (13.4H, $OCH_2$), 6.03 (Si—CH═ and unreacting olefin proton), 7.07 (br, 6.7H, Ar-CH═), 7.53 (13.4H, Ar-H), 7.68 (13.4H, Ar-H), 8.07 (26.8H, Ar-H). $^{13}$C-NMR (100 MHz, $CDCl_3$, $\delta$, ppm): 164, 156, 131, 129, 127, 123, 97, 67, 31, 29, 28, 22, 14. $^{29}$Si-NMR (79.49 MHz, $CDCl_3$, $\delta$, ppm): −79.22 (Si—C), −81.17 (Si—C). Anal. Calcd for $C_{170}H_{191}O_{26}N_{14}Si_8$ (hept-substituted cube): C, 66.51; H, 6.23; N, 6.39; Found (%): C, 66.76; H, 6.29; N, 6.39.

## RESULTS AND DISCUSSION

### Preparation and Solubility of Hybrids

The synthesis of all hybrids is outlined in Scheme 1. The reactions were very straightforward using commercially available OVS as one of the starting materials. To separate the resulting products, we had once tried to use gel permeation chromatography (GPC) method. As the hydrodynamic volumes of the different substituted species are quite similar, the GPC is unable to separate.[16,28] However, GPC in THF revealed single peak with similar peak positions for three hybrids, suggesting no reactants and core breakdown.[16,28] The solubility of the hybrids was also evaluated. The result showed that the hybrids of **P1–P3** are soluble in common organic solvents such as $CHCl_3$, $CH_2Cl_2$, toluene, and THF. Meanwhile, the hybrids also possessed excellent film-forming property.

### Structural Characterization

Figure 1 shows the FTIR spectra of OVS, **M1–M3**, and **P1–P3**. The FTIR spectrum of OVS shows three major characteristic peaks at 3066 $cm^{-1}$ (═C—H stretching), 1611 $cm^{-1}$ (C═C stretching), and 1112 $cm^{-1}$ (Si—O—Si stretching) and that of **M3** (take **M3** and **P3** as an example for discussion) shows a set of aromatic groups stretching absorption bands. The strong characteristic absorptions of Si—O—Si (1112 $cm^{-1}$) and the aromatic group stretching vibration absorption bands emerge in the spectrum of the hybrid **P3**, suggesting that the POSS cage may be incorporated into the oxadiazole units to obtain a new hybrid.[24] Similar results are also found in the spectra of **P1** and **P2**.

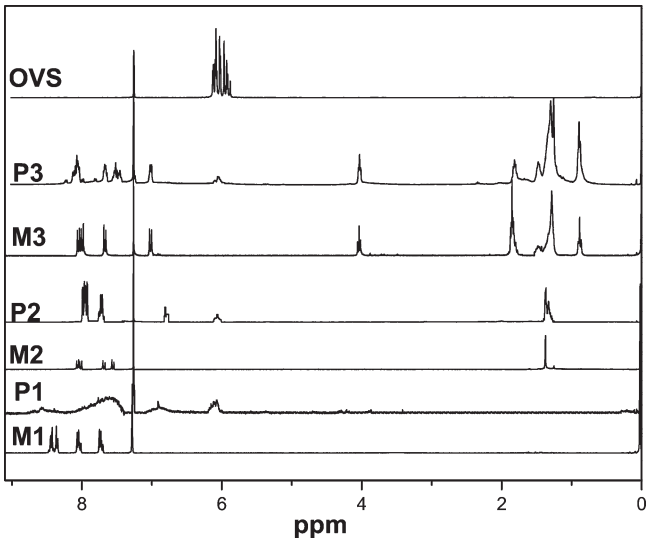


**Figure 2.** $^{1}$H-NMR spectra of OVS, **M1–M3** and **P1–P3**.

Figure 2 displays the $^{1}$H-NMR spectra of OVS, **M1–M3**, and **P1–P3** in chloroform-*d*. The absorption of OVS shows a set of characteristic olefin proton absorption peaks located at $\delta = 5.8$–6.2 ppm. Nevertheless, the $^{1}$H-NMR spectrum of the hybrid **P3** shows a weaker absorption at $\delta = 6.03$ ppm, belonging to the protons of the Si—C*H*═ and unreacting olefin proton absorption in OVS. Meanwhile, a new peak at $\delta = 7.07$ is found, which is ascribed to the absorption of the olefin proton linking to aromatic group, indicating that the oxadiazole groups are covalently attached to the POSS core to form the molecular dispersed organic–inorganic hybrids.[11,24,26] Similar result is also found in the spectra of **P2**. The absorption of aromatic proton in **P1** shows a broader distribution, which may be due to the polysubstitution products presenting in **P1**.

Figure 3 shows the $^{29}$Si-NMR spectra of OVS and **P1–P3**. As shown in Figure 3, a single peak at −81.15 ppm emerges in

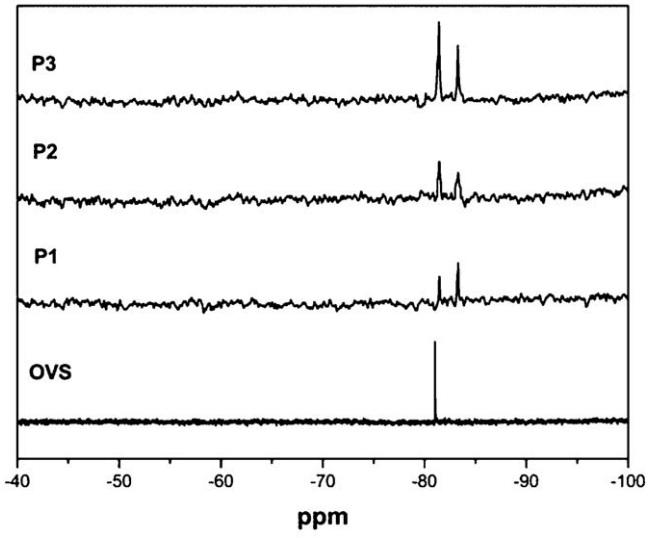


**Figure 3.** $^{29}$Si-NMR spectra of **P1–P3** and OVS.

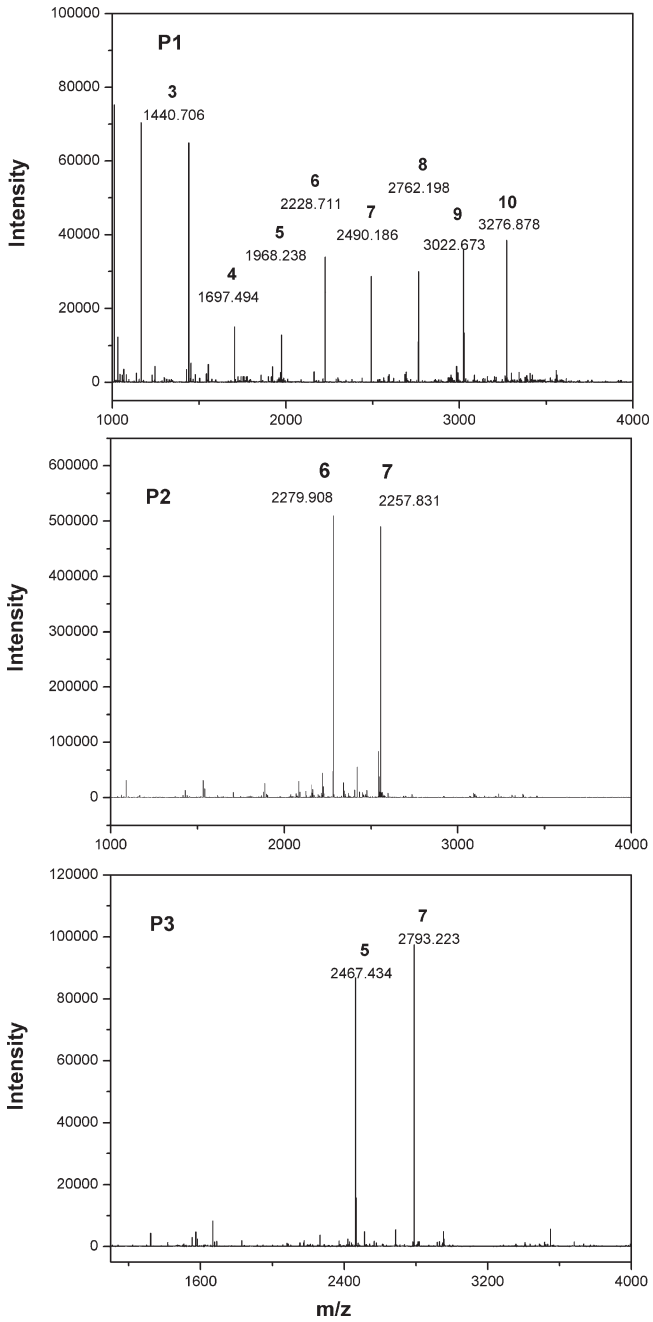


**Figure 4.** MALDI-TOF spectra of **P1–P3**.

OVS, indicating a symmetrical molecule and one silicon environment.[8,27] **P1–P3** displays major peaks at −79.46, −79.66, and −79.22 ppm, respectively. The primary Si peaks result from Si-vinyl groups with oxadiazole substituent.[11,24,28] The hybrids show minor peaks at −81.22, −81.30, and −81.17 ppm, respectively, attributing to the unsubstituted vinyl groups, and the values are close to −81.15 ppm, as mentioned above in OVS.

The propensity of the hybrids (**P1–P3**) was studied by MALDI-TOF. As indicated in Figure 4, the MALDI-TOF results show a distribution of **P1** with pulling electron group ranged from 3 to 10 substitutions,[28] with 9 and 10 being indicative of disubstituted vinyl groups. The result matches with the broader aromatic proton absorption peaks in the $^1$H-NMR. However, **P2** presents only 6 and 7 substitutions, and **P3** shows only 5 and 7 arms, which may be pushing electron groups limiting the maximum substitutions to eight. It might hint that the substitutions of hybrids with conjugated linkage were not affected by the steric factors[16,28] and that the electronic effects of terminal groups had obvious influence on the arm numbers of hybrids, which provides the potential strategy for the preparation of POSS-based hybrids with 3D structures by the variety of the substituent groups. Elemental analyses of the **P1**, **P2**, and **P3** indicated that about 7, 6.5, and 6.7 oxadiazole chromophores were attached to each cube average, respectively. It is consistent with the results of MALDI-TOF of **P1–P3**.

## Optical Properties

The UV–vis absorption and fluorescence emission spectra of **P1–P3** are shown in Figure 5. The maximum absorption wavelengths of **P1–P3** are located at the range of 291–295 nm, corresponding to the transition of the oxadiazole units.[24] The maximum absorption wavelengths and optical band gaps ($E_g$) for the hybrids are summarized in Table I.

Figure 5 illustrates the fluorescence emission spectra of **P1–P3** in THF solutions ($1 \times 10^{-5}$ mol L$^{-1}$). The emission spectra properties for the hybrids are summarized in Table I. The results show that **P1–P3** has intense blue–violet emission. The PL quantum yield ($\Phi_f$) was determined by using quinine sulfate in 0.10 mol L$^{-1}$ $H_2SO_4$ as the standard.[29] $\Phi_f$ values of **P2** and **P3** are up to 43% and 51%, respectively, which is much larger than that of reported nanocomposite $O_8$OVS with similar chromophore (1%).[28] The reason may be the cubic core structure functionalized as a stable spacer for separating organic arms (luminescent centers) to achieve quantum confinement effects,[27] and the 3D structure with rigid linkage between the POSS core and oxadiazole groups suppressed intramolecular and intermolecular $\pi$–$\pi$ interactions.[3,24,37,38] In addition, the *tert*-butyl or alkoxy chains are grafted at terminal in **P2** or **P3**, respectively, which increase the torsion energy barrier of diaryl-oxadiazole and minimizing the rotating of arms, and further reduce the intermolecular interaction.[3,27] On the other hand, **P2** and **P3**

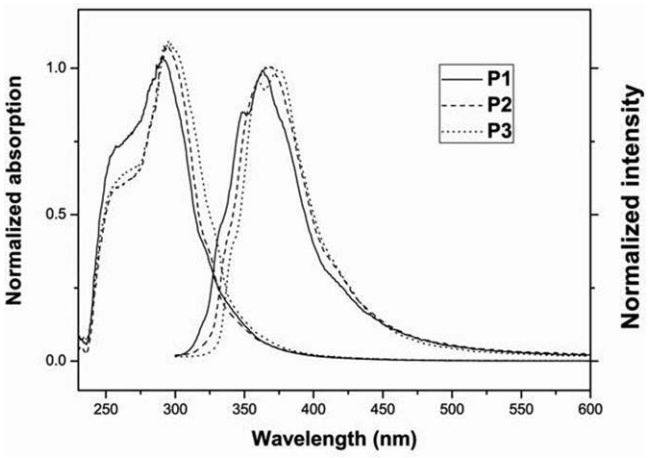


**Figure 5.** UV–vis absorption ($2 \times 10^{-4}$ mol L$^{-1}$) and fluorescence emission ($1 \times 10^{-5}$ mol L$^{-1}$) spectra of **P1–P3** in THF solution.

**Table I.** The Properties of the 3D Hybrids P1–P3

| Sample | $\lambda_{abs}$[a] (nm) | $\lambda_{PL}$[b] (nm) | $\Phi_f$[c] | $E_{onset}$ (V) | $E_g$[d] (eV) | LUMO[e] (eV) | HOMO[f] (eV) |
|---|---|---|---|---|---|---|---|
| **P1** | 291 | 363 | 0.16 | −0.70 | 3.28 | −3.70 | −6.98 |
| **P2** | 294 | 367 | 0.43 | −1.00 | 3.57 | −3.40 | −6.97 |
| **P3** | 295 | 375 | 0.51 | −1.07 | 3.61 | −3.33 | −6.94 |

[a] Determined in THF solution ($2 \times 10^{-4}$ mol $L^{-1}$).
[b] Measured in THF solution ($1 \times 10^{-5}$ mol $L^{-1}$), excited at wavelength of the maximum absorbance.
[c] Quantum yields determined by using a dilute quinine sulfate in 0.10 mol $L^{-1}$ $H_2SO_4$ as the standard ($\Phi_f = 0.546$).[29]
[d] Estimated from the onset wavelength of UV-vis absorption spectra in film.
[e] Estimated from the onset of the cathode current.
[f] $E_{HOMO} = E_{LUMO} - E_g$.

with pushing electron groups have only two types of substitutions, and the higher purity as well as relatively symmetric structures are helpful to the enhancement of the fluorescence quantum yield.[28] The quantum yield value of **P1** is only 16%. When compared with that of **P2** and **P3**, the decrease is due to the pulling electron effect of the nitryl group in **P1**.[3,38]

For elucidating this, PL spectra of the annealed film of **P3** from 50 to 110°C in air were performed. To make the comparison, PL spectrum of **P3** at 20°C was measured at the same condition and is shown in Figure 6 (Curve **a**). As shown in Figure 6, the blue emission peaks of **P3** were located at 445 and 420 nm at different temperatures (from 20 to 110°C). The PL spectra profile and the emission intensity of those annealed films are lightly weakened, suggesting slight tendency toward aggregation in the solid state.[16,28] Figure 7 shows the electron absorption spectra of **P3** in annealed film. As shown in Figure 7, under the annealing temperatures at 20, 50, 80, 110°C, the maximum absorption peaks of **P3** are located at 296, 300, 304, and 309 nm, respectively. The maximum absorption shows a red-shift from 296 to 309 nm with an increase in the annealing temperature, indicating that a slight aggregation occurred in annealing films.[39,40] When compared with the flat molecules such as PTCDI,[41,42] nevertheless, the red-shifted absorption of **P3** led by the aggregation is not significant. Similar phenomenon was also found in an oxadiazole-containing cyclotriphosphazene core hybrid molecule with no flat structure.[40] The result further demonstrated that the hybrid with 3D molecular structure can efficiently restrain intramolecular and intermolecular $\pi$–$\pi$ interactions.[24]

### Electrochemical Properties

Cyclic voltammetry was used to investigate the redox behavior of **P1–P3** and to estimate the lowest unoccupied molecular orbital (LUMO) energy levels based on the equation $E_{LUMO} = -(E_{onset}^{red} + 4.4)$ (eV)[43,44] and the highest occupied molecular orbital (HOMO) energy levels based on $E_{LUMO}$ and $E_g$. The measurement of the onset potentials and the preparation of hybrid films were according to the method proposed in Refs. 43 and 44.

Figure 8 shows the CV curves of n-doping process of **P1–P3**. The energy levels of the hybrids are listed in Table I. During the cathodic scan, the hybrids exhibit a quasi-reversible reduction processes, and the onsets occur at −0.70, −1.00, and −1.07 eV for **P1**, **P2**, and **P3**, corresponding to $E_{LUMO}$ values at −3.70, −3.40, and −3.33 eV, respectively. The $E_{LUMO}$ of **P1** with nitryl (pulling electron group) is the lowest and that of **P3** with alkyoxy (pushing electron groups) is the highest in the three hybrids, suggesting that the pulling electron group may improve the electron injection from the metal electrode.[2] Thus, the

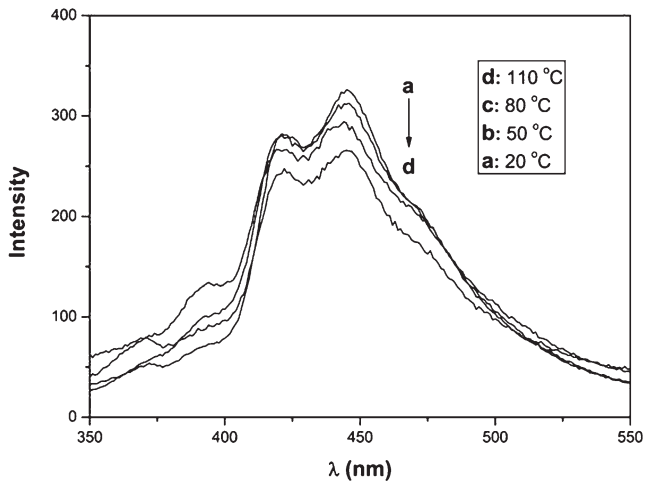


**Figure 6.** PL spectra of **P3** in films after annealing treatment.

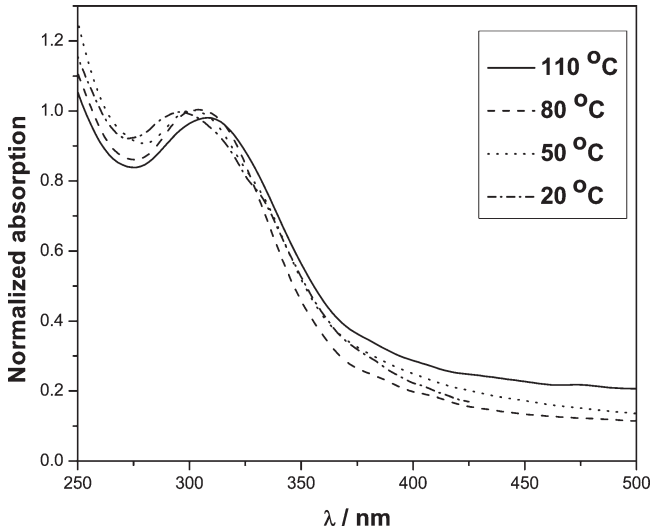


**Figure 7.** Electron absorption spectra of **P3** in films after annealing treatment.

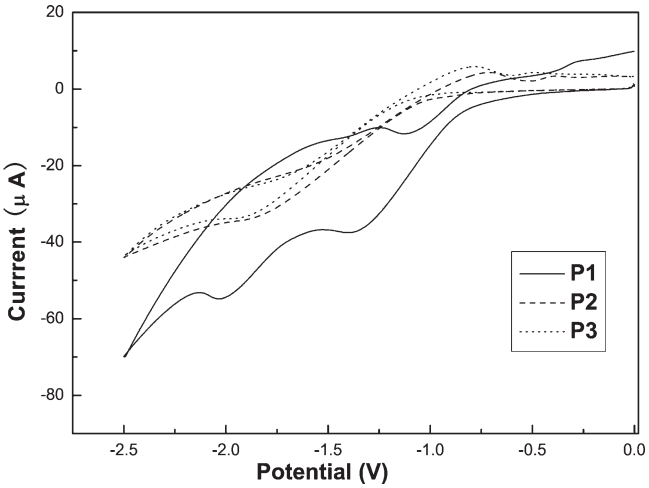


**Figure 8.** Cyclic voltammogram curves of **P1–P3** (in $CH_3CN$/supporting electrolyte: 0.10 × mol $L^{-1}$ TBAP; scan rate: 50 mV $s^{-1}$).

electron injection ability of the hybrids can be effectively modulated by varying molecular design and architecture.

## CONCLUSIONS

In conclusion, a series of oxadiazole-containing 3D hybrid materials were successfully designed and efficiently synthesized. The combination of the inorganic POSS core and oxadiazole chromophores using Heck reaction significantly endows the resultant hybrids with 3D structure, higher value of PL quantum yield ($\Phi_f$), and good electron injection properties. The variety of substitute groups had obvious influence on the arm numbers of hybrids and optical properties as well as the properties of electron injection (or $E_{LUMO}$). This work provides the potential strategy for the preparation of nanocomposite materials that combined the organic molecular chromophores with the POSS core using a rigid link for LED applications.

## ACKNOWLEDGMENTS

This work was supported by the National Natural Science Fund of China (Grant Nos. 21271035, 21102001, and 51003013), the State Key Laboratory for Modification of Chemical Fibers and Polymer Materials (Grant No. LK1008), the Key Subject of Chizhou University (Grant No. 2011XK04), and the Anhui Provincial University Natural Science Foundation (Grant No. KJ2013B174).

## REFERENCES

1. Hughes, G.; Bryce, M. R. *J. Mater. Chem.* **2005**, *15*, 94.
2. Kulkarni, A. P.; Tonzola, C. J.; Babel, A.; Jenekhe, S. A. *Chem. Mater.* **2004**, *16*, 4556.
3. Xiao, Y.; Liu, L.; He, C.; Chin, W. S.; Lin, T.; Mya, K. Y.; Huang, J.; Lu, X. *J. Mater. Chem.* **2006**, *9*, 829.
4. Wang, X.; Guan, S.; Xu, H.; Su, X.; Zhu, X.; Li, C. *J. Polym. Sci. Part A: Polym. Chem.* **2010**, *48*, 1406.
5. Kanibolotsky, A. L.; Perepichka, I. F.; Skabara, P. *J. Chem. Soc. Rev.* **2010**, *39*, 2695.
6. Eaton, P. E. *Angew. Chem. Int. Ed. Engl.* **1992**, *31*, 1421.
7. Roll, M. F.; Asuncion, M. Z.; Kampf, J.; Laine, R. M. *ACS Nano* **2008**, *2*, 320.
8. Sanchez, C. M.; Belleville, P.; Popalld, M.; Nicoleab, L. *Chem. Soc. Rev.* **2011**, *40*, 696.
9. Wang, F.; Lu, X.; He, C. *J. Mater. Chem.* **2011**, *21*, 2775.
10. Cordes, D. B.; Lickiss, P. D.; Rataboul, F. *Chem. Rev.* **2010**, *110*, 2081.
11. Su, X.; Guang, S.; Li, C.; Xu, H.; Liu, X.; Wang, X.; Song, Y. *Macromolecules* **2010**, *43*, 2840.
12. Su, X.; Guang, S.; Xu, H.; Liu, X.; Li, S.; Wang, X.; Deng, Y.; Wang, P. *Macromolecules* **2009**, *42*, 8969.
13. Sulaiman, S.; Bhaskar, A.; Zhang, J.; Guda, R.; Goodson, T.; Laine, R. M. *Chem. Mater.* **2008**, *20*, 5563.
14. Fan, H.; He, J.; Yang, R. *J. Appl. Polym. Sci.* **2013**, *127*, 463.
15. Wang, X.; Ervithayasuporn, V.; Zhang, Y.; Kawakami, Y. *Chem. Commun.* **2011**, *47*, 1282.
16. Sellinger, A.; Tamaki, R.; Laine, R. M.; Ueno, K.; Tanabe, H.; Williams, E.; Jabbour, G. E. *Chem. Commun.* **2005**, 3700.
17. Lo, M. Y.; Zhen, C.; Lauters, M.; Jabbour, G. E.; Sellinger, A. *J. Am. Chem. Soc.* **2007**, *129*, 5808.
18. Jiang, C.; Zhang, C.; Bao, X.; Liu, B.; Mu, J. *J. Appl. Polym. Sci.* **2013**, *129*, 3162.
19. Xu, N.; Stark, E. J.; Carver, P. I.; Sharps, P.; Hu, J.; Hartmann-Thompson, C. *J. Appl. Polym. Sci.* **2013**, *130*, 3849.
20. Zhang, C.; Laine, R. M. *J. Am. Chem. Soc.* **2000**, *122*, 6979.
21. Sellinger, A.; Laine, R. M. *Macromolecules* **1996**, *29*, 2327.
22. Xu, H.; Gao, X.; Guang, S.; Chang, F. C. *Chin. Chem. Lett.* **2005**, *16*, 41.
23. Miao, Q. J.; Fang, Z.-P.; Cai, G. P. *Catal. Commun.* **2003**, *4*, 637.
24. Wang, X.; Guang, S.; Xu, H.; Su, X.; Lin, N. *J. Mater. Chem.* **2011**, *21*, 12941.
25. Sellinger, A.; Laine, R. M. *Chem. Mater.* **1996**, *8*, 1592.
26. Cheng, G.; Vautravers, N. R.; Morris, R. E.; Cole-Hamilton, D. *J. Org. Biomol. Chem.* **2008**, *6*, 4662.
27. He, C. B.; Xiao, Y.; Huang, J. C.; Lin, T. T.; Mya, K. Y.; Zhang, X. H. *J. Am. Chem. Soc.* **2004**, *126*, 7792.
28. Lo, M. Y.; Ueno, K.; Tanabe, H.; Sellinger, A. *Chem. Rec.* **2006**, *6*, 157.
29. Crosby, G. A.; Demas, J. N. *J. Phys. Chem.* **1971**, *75*, 991.
30. Cho, H. J.; Hwang, D. H.; Lee, J. I.; Jung, Y. K.; Park, J. H.; Lee, J.; Lee, S. K.; Shim, H. K. *Chem. Mater.* **2006**, *18*, 3780.
31. Wang, C.; Palsson, L.-O.; Batsanov, A. S.; Bryce, M. R. *J. Am. Chem. Soc.* **2006**, *128*, 3789.
32. Augustine, J. K.; Vairaperumal, V.; Narasimhan, S.; Alagarsamy, P.; Radhakrishnan, A. *Tetrahedron* **2009**, *65*, 9989.
33. Backhall, A.; Brydon, D. L.; Javaid, K.; Sagar, A. J. G.; Smith, D. M. *J. Chem. Res.* **1984**, 3485.
34. Wang, X.; Wu, J.; Xu, H.; Wang, P.; Tang, B. Z. *J. Polym. Sci. Part A: Polym. Chem.* **2008**, *46*, 2072.

35. Yin, S.; Xu, H.; Su, X.; Li, G.; Song, Y.; Lam, J. W. Y.; Tang, B. *J. Polym. Sci. Part A: Polym. Chem.* **2006**, *44*, 2346.
36. Tang, B. Z.; Kong, X.; Wan, X.; Feng, X. D. *Macromolecules* **1997**, *30*, 5620.
37. Jin, S. H.; Kim, M. Y.; Kim, J. Y.; Lee, K.; Gal, Y. S. *J. Am. Chem. Soc.* **2004**, *126*, 2474.
38. Pu, K.-Y.; Luo, Z.; Li, K.; Xie, J.; Liu, B. *J. Phys. Chem. C.* **2011**, *115*, 13069.
39. Huang, H.; He, Q.; Song, Y.; Lin, H.; Yang, J.; Bai, F. *Polym. Adv. Technol.* **2003**, *14*, 309.
40. Liu, S.-Z.; Wu, X.; Zhang, A.-Q.; Qiu, J.-J.; Liu, C.-M. *Langmuir* **2011**, *27*, 3982.
41. Balakrishnan, K.; Datar, A.; Naddo, T.; Huang, J.; Oitker, R.; Yen, M.; Zhao, J.; Zang, L. *J. Am. Chem. Soc.* **2006**, *128*, 7390.
42. Zang, L.; Che, Y.; Moore, J. S. *Acc. Chem. Res.* **2008**, *41*, 1596.
43. Meng, H.; Yu, W. L.; Huang, W. *Macromolecules* **1999**, *32*, 8841.
44. Leeuw, D. M. D.; Simenon, M. M. J.; Brown, A. R.; Einerhand, R. E. F. *Synth. Met.* **1997**, *87*, 53.